UNCLASSIFIED

AD 297 895

Reproduced
by the

ARMED SERVICES TECHNICAL INFORMATION AGENCY
ARLINGTON HALL STATION
ARLINGTON 12, VIRGINIA

UNCLASSIFIED

63-2-5

TR-1087

FLUID AMPLIFICATION

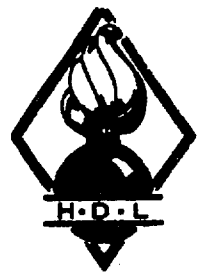## 5. Jet Attachment Distance as a Function of Adjacent Wall Offset and Angle

Sheldon G. Levin

Francis M. Manion

31 December 1962

HARRY DIAMOND LABORATORIES
FORMERLY: DIAMOND ORDNANCE FUZE LABORATORIES
ARMY MATERIEL COMMAND
WASHINGTON 25. D.C.

HARRY DIAMOND LABORATORIES

Robert W. McEvoy
LtCol, Ord Corps
Commanding

B. M. Horton
Technical Director

MISSION

The mission of the Harry Diamond Laboratories is:

(1) To perform research and engineering on systems for detecting, locating, and evaluating targets; for accomplishing safing, arming, and munition control functions; and for providing initiation signals: these systems include, but are not limited to, radio and non-radio proximity fuzes, predictor-computer fuzes, electronic timers, electrically-initiated fuzes, and related items.

(2) To perform research and engineering in fluid amplification and fluid-actuated control systems.

(3) To perform research and engineering in instrumentation and measurement in support of the above.

(4) To perform research and engineering in order to achieve maximum immunity of systems to adverse influences, including counter-measures, nuclear radiation, battlefield conditions, and high-altitude and space environments.

(5) To perform research and engineering on materials, components, and subsystems in support of above.

(6) To conduct basic research in the physical sciences in support of the above.

(7) To provide consultative services to other Government agencies when requested.

(8) To carry out special projects lying within installation competence upon approval by the Director of Research and Development, Army Materiel Command.

(9) To maintain a high degree of competence in the application of the physical sciences to the solution of military problems.

FLUID AMPLIFICATION

5. Jet Attachment Distance as a Function of
Adjacent Wall Offset and Angle

Sheldon G. Levin

Francis M. Manion

FOR THE COMMANDER:
Approved by

R. D. Hatcher
R. D. Hatcher
Chief, Laboratory 300

CONTENTS

LIST OF ILLUSTRATIONS

4

ABSTRACT

Attachment of a submerged, incompressible, two-dimensional, turbulent jet to an adjacent straight wall (Coanda effect) is analyzed. Parametric equations are developed that predict the point at which the jet attaches as a function of wall angle and offset distance. Computer solutions were obtained for several sets of conditions. Experiments were conducted with both air and water jets at Mach 0.5 equivalent, and results agree well with corresponding computer solutions when the jet spread parameter is also treated as a function of offset distance and wall angle. The equations provide an analytic method, independent of the particular fluid, for predicting the attachment distance, and should be helpful in designing elements based on the Coanda effect; e.g., the fluid flip-flops or bistable elements.

1. INTRODUCTION

The steady-state deflection and attachment of a jet to nearby surface has been referred to as the Coanda effect. The effect with respect to two-dimensional flow is of interest since two-dimensional flow is approximated in many fluid devices where the flow is constrained between two opposing parallel flat plates, and the proper design of many elements using the Coanda effect requires a means for calculating the attachment distance as wall angle and offset distance are varied.

Borque and Newman (ref 1) as well as Sawyer (ref 2) discuss the deflection and reattachment of a two-dimensional, submerged, incompressible, turbulent jet to an adjacent flat plate, and develop equations to predict the attachment distance as a function of the distance that the wall is offset from the nozzle exit, or, alternatively, as a function of the angle between the wall with zero offset and the axis of the nozzle. A study was initiated to develop a more general expression of attachment distance as a function of both parameters. The study included a theoretical analysis and derivation, computer solutions, and tests with air and water jets.

2. THEORETICAL DEVELOPMENT

2.1 Analytic Base

The Coanda effect, as discussed here, arises as follows. A submerged jet (fig. 1) entrains fluid by means of viscous interaction between the moving stream and the quiescent surrounding fluid. If a wall is located such that the replacement flow is impeded, the static pressure in the fluid between the jet and wall decreases, and the pressure differential across the jet deflects the jet towards the wall. The pressure differential is self-reinforcing until the jet is deflected far enough to attach to the wall. A bubble of reduced static pressure is inclosed between the jet stream and wall maintaining the attachment.

A steady-state flow pattern arises where the mass entrained by the jet from the bubble is returned to the bubble near the attachment point.

The analytic development of a general expression describing the steady-state flow pattern requires the following assumptions:

(a) The jet flow is incompressible and two-dimensional.

(b) Jet velocity is uniform at the nozzle exit.

(c) The jet velocity is independent of the reduced pressure in the bubble.

(d) The pressure within the separation bubble is uniform.

(e) Jet momentum flux is conserved, i.e., drag losses due to constraining plates are neglected.

(f) The centerline of the jet is a circular arc of radius R.

(g) The nozzle width is small compared with R; and the attachment-wall length is long compared with the nozzle width.

(h) The jet exhibits turbulent flow after emerging from the nozzle; i.e., the Reynolds number is high.

(i) Changes in the jet structure due to the centrifugal force of curvature are negligible.

2.2 Notation

Figure 1 illustrates the jet model. The notation used in figure 1 and in the derivation is as follows:

D = distance from attachment wall to the side of the nozzle (ft)

J = jet momentum flux per unit depth (lbf/ft)

p_o = stagnation pressure of the fluid supplying the jet (lbf/ft^2)

p_B = static pressure of fluid in bubble (lbf/ft^2)

p_∞ = static pressure of fluid surrounding the jet (lbf/ft^2)

Q = volume flow (ft^3/sec)

Q_e = volume flow at nozzle exit (ft^3/sec)

Q_T = total volume flow at a distance s from the nozzle exit (ft^3/sec)

R = radius of a theoretical circular arc described by the jet centerline (ft)

s = arbitrary distance along the jet centerline from the nozzle exit (ft)

s_o = distance from the hypothetical (apparent) origin of the jet to the nozzle exit.

t = parameter from Goertler's equation for jet velocity profile (dimensionless)

6

u = jet stream velocity (fps)

u_e = uniform jet stream velocity at the exit (fps)

u_o = jet stream velocity at the centerline (fps)

w = nozzle width (ft)

y = distance from the jet centerline to an arbitrary point measured on a line normal to the centerline (ft)

y' = distance from the jet streamline that passes through the attachment point to the jet centerline, measured on a line normal to the centerline

x = distance from the attachment point to the offset wall measured along the attachment wall (ft)

α = angle between the attachment wall and a line parallel to the nozzle axis (rad or deg)

θ = angle between the jet centerline and the attachment wall (rad or deg)

ρ = density of the fluid (lbm/ft^3)

σ = spread parameter for a free turbulent jet (dimensionless)

g_c = 32.2 lbm-ft/sec-lbf
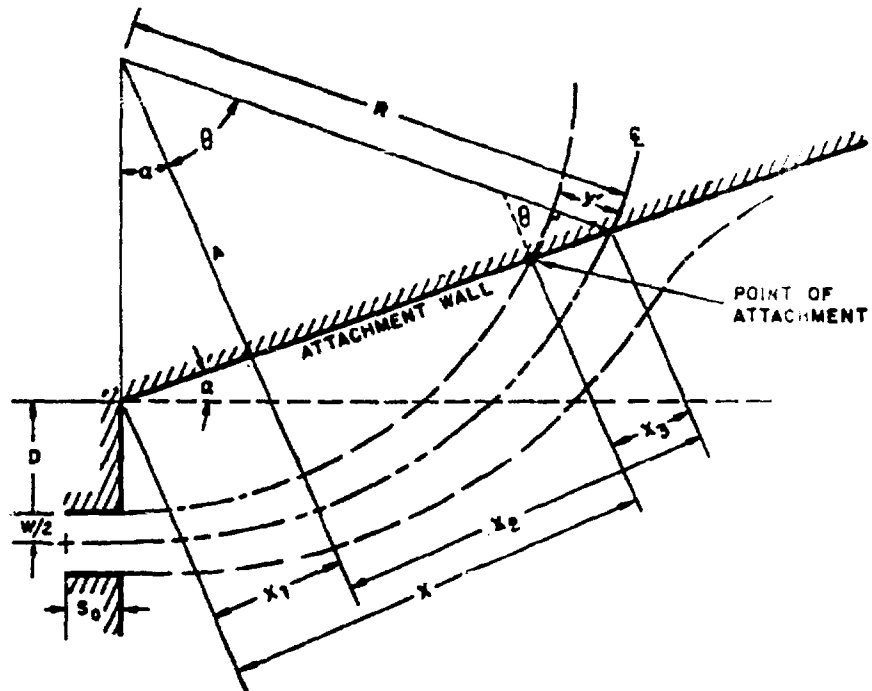
Figure 1. Mathematical model of the attachment of a two-dimensional jet to an offset, inclined adjacent wall.

2.3 Derivation of Equations

2.3.1 Parameter (t)

The parameter t, which is taken from the velocity-profile equation given by Goertler (ref 3), is derived as follows (fig. 1):

Goertler gives the jet stream velocity u as a function of the distance s the jet has traveled, the distance y from the centerline, and the jet centerline velocity u_o at a distance s from the nozzle exit, thus,

$$u = u_o \operatorname{sech}^2 \left(\frac{\sigma y}{s + s_o} \right) \tag{1}$$

$$u_o = \left[\frac{3J\sigma g_c}{4\rho(s + s_o)} \right]^{1/2}$$

where s_o is the distance from the nozzle exit to the apparent jet origin (the point from which the jet appears to emanate) y is an arbitrary distance from the centerline, σ is the jet spread parameter, and J is the jet momentum flux.

The velocity profile at the nozzle exit is uniform (fig. 2a) by assumption. A representative jet velocity profile at s per Goertler's expression is illustrated in figure 2b.
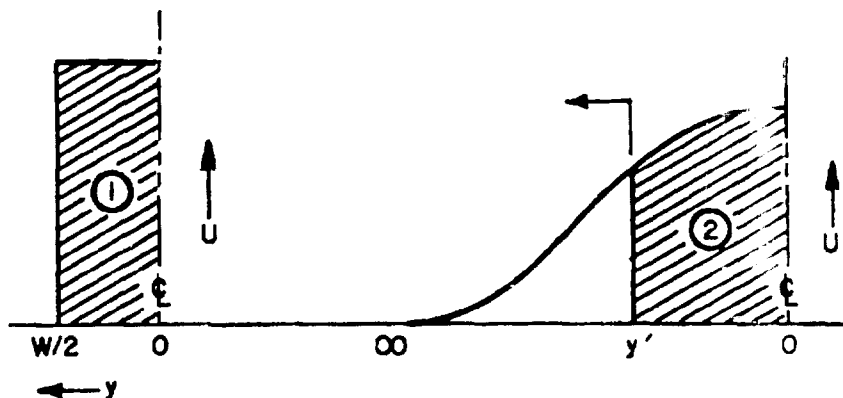
(a) Jet stream velocity profile   (b) Jet stream velocity profile
    assumed at s = 0   at a distance s > 0 per
                              Goertler's expression

Figure 2. Jet stream velocity profiles.

In general, volume flow is not conserved, but by assumption, there exists a line of constant volume flow which is called the attachment streamline. The attachment streamline is a distance w/2 from the jet centerline at the nozzle exit and a distance y' from the centerline at a distance s from the nozzle. The fluid is incompressible and two dimensional by assumption; hence, one half the jet volume flow is

$$\frac{Q}{2} = \int_0^{y'} u \, dy$$

To solve for s_o, one half the volume flow $Q_e/2$ at the nozzle exit is first assumed to be equal to one half the volume flow Q/2 at s > 0 using Goertler's expression, i.e.,

$$\frac{Q_e}{2} = \frac{Q}{2} \quad \text{or} \quad u_e \frac{w}{2} = \int_0^{y'} u \, dy \qquad (2)$$

where w is the nozzle width and u_e is the velocity at the nozzle exit. Substituting (1) into (2)

$$\int_0^{y'} \left[\frac{3J\sigma g_c}{4\rho(s + s_o)} \right]^{1/2} \text{sech}^2 \left(\frac{\sigma y}{s + s_o} \right) dy = u_e \frac{w}{2}$$

By integrating and noting that tanh 0 = 0,

$$\left[\frac{3}{4} \frac{J\sigma g_c}{\rho(s + s_o)} \right]^{1/2} \left(\frac{s + s_o}{\sigma} \right) \tanh \left(\frac{\sigma y'}{s + s_o} \right) = u_e \frac{w}{2}$$

which simplifies to

$$\left[\frac{3}{4} \frac{J(s + s_o)g_c}{\rho\sigma} \right]^{1/2} \tanh \left(\frac{\sigma y'}{s + s_o} \right) = u_e \frac{w}{2} \qquad (3)$$

which is an expression for the volume flow for half the stream at the nozzle exit. Since the jet momentum flux at the nozzle exit is $J = \frac{\rho u_e^2 w}{g_c}$, the normalized volume flow for half the stream becomes

$$\left[\frac{3(s + s_o)}{w\sigma} \right]^{1/2} \tanh \left(\frac{\sigma y'}{s + s_o} \right) = 1$$

Then the dimensionless parameter t is defined as

$$t = \tanh \frac{\sigma y}{s + s_o} \tag{4}$$

and

$$t'^2 = \tanh^2 \left(\frac{\sigma y'}{s + s_o} \right) = \frac{w\sigma}{3(s + s_o)} \tag{5}$$

which is the equation of the streamline.

      Figure 3 shows that Goertler's equation does not adequately represent the volume flow at the nozzle exit. However, the approximation is made: the volume flow at the nozzle exit $u_e(w/2)$ is forced to be equal to the volume flow at the nozzle exit given by Goertler's equation $\int_0^{\infty} u\,dy$. This permits an evaluation of s_o.

ASSUMED FLOW AT NOZZLE EXIT

PREDICTED FROM GOERTLER'S PROFILE EQUATION
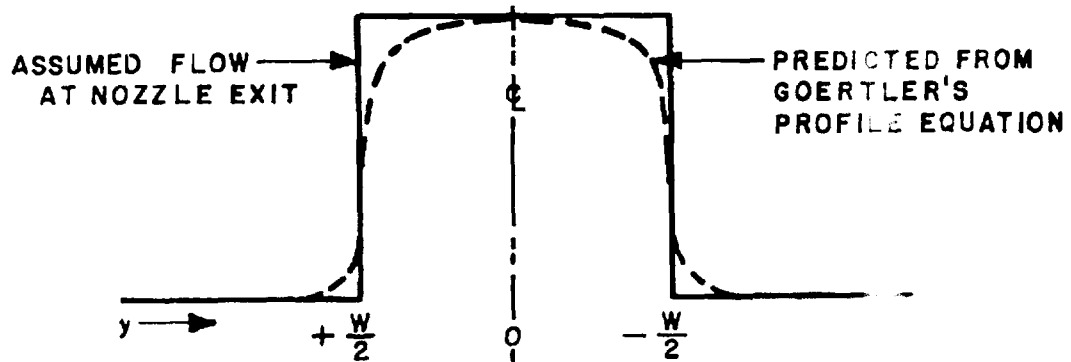
Figure 3. Comparison of Goertler's equation prediction with assumed flow at nozzle exit.

$$\int_0^{\infty} u\,dy = u_e \frac{w}{2}$$

and proceeding as with equation (2)

$$\left[\frac{3}{4}\frac{J(s+s_0)g_0}{\rho\sigma}\right]^{1/2}\tanh\left(\frac{\sigma y}{s+s_0}\right)\Bigg|_0^\infty = u_e\frac{W}{2}$$

$$\left[\frac{3}{4}\frac{J(s+s_0)g_c}{\rho\sigma}\right]^{1/2} = u_e\frac{W}{2} \tag{6}$$

At the nozzle exit $s = 0$ and $J = \dfrac{\rho u_e^2 W}{g_c}$

then

$$\left[\frac{3}{4}\frac{\rho u_e^2 W s_0 g_c}{4\rho\sigma}\right]^{1/2} = u_e\frac{W}{2}$$

which becomes

$$s_0 = \frac{\sigma W}{3} \tag{7}$$

Substituting (7) into (5) yields

$$\frac{3s}{\sigma W} = \frac{1}{t'^2} - 1 \tag{8}$$

for the attachment streamline.

2.3.2 Attachment Angle

Two approaches that may be used to express the attachment angle θ as a function of t are illustrated in figure 4. The first
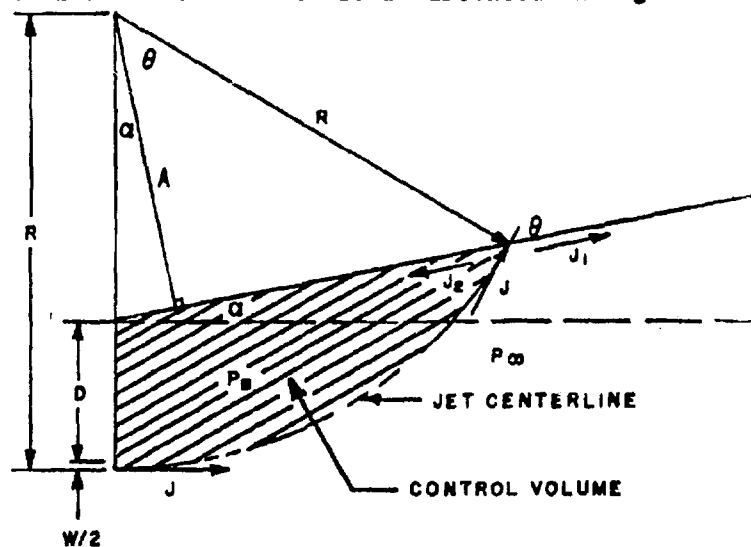
Figure 4. Mathematical model for control-volume and attachment-point theories.

approach evaluates the forces (J, J_1, and J_2) acting at the attachment point and assumes that the momentum flux component parallel to the wall is conserved. This representation of the attachment mechanism will be called the attachment-point model. The second approach considers the forces due to ($p_\infty - p_B$) acting on the control volume inclosed by the centerline of the jet, the attachment wall and offset wall, shown as the shaded region in figure 4. The two models considered are attempts to represent the mechanism of attachment. There seemed no reason to prefer either model, and both were developed.

Attachment-Point Model—An expression for θ in terms of t is obtained as follows: From figure 4 one can write

$$J_1 - J_2 = J \cos \theta \tag{9}$$

The J's can be written as integrals of the form

$$\int \rho u^2 dy$$

Using the Goertler equation (1), this becomes

$$\int \rho u^2 dy = \rho \left(\frac{3J\sigma}{4\rho(s + s_o)} \right) \left(\frac{s + s_o}{\sigma} \right) \int \operatorname{sech}^4 \left(\frac{\sigma y}{s+s_o} \right) d \left(\frac{\sigma y}{s+s_o} \right)$$

Integrating and substituting the value of t from (4)

$$J_2 = \int_{y'}^{\infty} \rho u^2 \, dy = \frac{J}{4} (3t - t^3) \Big|_{y'}^{\infty}$$

Since $t = \tanh \dfrac{\sigma y}{s + s_o}$, $\tanh 0 = 0$, and $\tanh \infty = 1$,

$$J_2 = \frac{J}{4} (3-1) - \frac{J}{4} (3t'-t'^3) = \frac{J}{2} - \frac{J}{4} (3t'-t'^3) \tag{10}$$

Now

$$J_1 = \int_{-\infty}^{y'} \rho u^2 dy = \int_{-\infty}^{0} \rho u^2 dy + \int_{0}^{y'} \rho u^2 dy$$

Since

$$J = \int_{-\infty}^{\infty} \rho u^2 dy$$

12

and since u is symmetric

$$\frac{J}{2} = \int_{-\infty}^{0} \rho u^2 dy = \int_{0}^{\infty} \rho u^2 dy$$

Thus

$$J_1 = \frac{J}{2} + \int_{0}^{y'} \rho u^2 dy$$

Proceeding as with J_2,

$$J_1 = \frac{J}{2} + \frac{J}{4}(3t' - t'^3) \tag{11}$$

Inserting the values of J_1 and J_2 from (10) and (11) into (9)

$$J \cos \theta = J \left(\frac{1}{2} + \frac{3}{4} t' - \frac{1}{4} t'^3\right) - J\left(\frac{1}{2} - \frac{3}{4} t' + \frac{1}{4} t'^3\right)$$

and finally

$$\cos \theta = \frac{3}{2} t' - \frac{t'^3}{2} \tag{12}$$

Control-Volume Model—The force equation states that the momentum flux returned to the low-pressure region p_B balances the pressure difference times the area normal to the wall. This can be expressed as

$$J \cos \alpha - J_1 = (p_\infty - p_B) \left(D + \frac{w}{2}\right) \cos \alpha \tag{13}$$

From figure 4

$$\cos \alpha = \frac{A}{R - D - w/2} \quad \text{and} \quad \cos \theta = \frac{A}{R}$$

thus

$$R - \frac{A}{\cos \alpha} = D + \frac{w}{2}$$

Substituting $\cos \theta = \frac{A}{R}$ gives

$$R\left(1 - \frac{\cos \theta}{\cos \alpha}\right) = D + \frac{w}{2} \tag{14}$$

13

Using (14) and the approximation $\Delta P = \frac{J}{R}$ (justified in appendix A) in (13)

$$J \cos \alpha - J_1 = (\frac{J}{R}) \; R \; (1 - \frac{\cos \theta}{\cos \alpha}) \cos \alpha$$

which simplifies to

$$\cos \alpha - \frac{J_1}{J} = \cos \alpha - \cos \theta$$

Hence

$$\cos \theta = \frac{J_1}{J} \tag{15}$$

which is equivalent to (9) with $J_2 = 0$.

Substituting the value of J_1/J from equation (11) gives

$$\cos \theta = \frac{\frac{J}{4} (3t' - t'^3) + \frac{J}{2}}{J} = \frac{1}{2} + \frac{3}{4} t' - \frac{t'^3}{4} \tag{16}$$

As in (12), $\cos \theta$ again involves only y, s, and σ, and not α. Equations (12) and (16) are the same as those obtained by Borque and Newman even though the wall angle α has been considered in this derivation.

Comparison of Models—Two different expressions for $\cos \theta$ as a function of t' have been derived. In the process, two expressions relating (J, J_1, J_2) and $\cos \theta$ have occurred.

attachment-point model: $J_1 - J_2 = J \cos \theta$ (9)

control-volume model: $J_1 = J \cos \theta$ (15)

The primary reason for this difference in (9) and (15) is that the difference of pressure $p_{\infty} - p_B = \Delta p$ was neglected in the attachment-point model. The reaction of the stream to J_2 tends to move the attachment point downstream, hence to increase x. The effect of Δp on the jet is to decrease x by shrinking the trapped bubble. Thus the consideration of Δp tends to reduce the magnitude of J_2. If the control volume model were more nearly correct—as measured by the discrepancy between the theory and experimental data—then one might conclude that the effect of Δp tends to cancel J_2. However if the attachment-point model agreed more closely with experiment data, then this would not be so.

14

2.3.3 Geometry of Attachment

Substituting (7) into (4)

$$\tanh^{-1} t' = \frac{\sigma y'}{s + \frac{\sigma w}{3}}$$

Then solving for y' and substituting the value of $3s/\sigma w$ from (8)

$$y' = \frac{3s + \sigma w}{3\sigma} \tanh^{-1} t' = \frac{w}{3}\left[\frac{1}{t'^2} - 1 + 1\right]\tanh^{-1} t'$$

Finally

$$y' = \frac{w}{3t'^2}\tanh^{-1} t' \tag{17}$$

For the case where s is the distance from the nozzle exit to the attachment point, (fig. 4)

$$s = R(\theta + \alpha) \tag{18}$$

and combining (8) and (18) yields

$$\frac{1}{t'^2} - 1 = \frac{3R(\theta + \alpha)}{\sigma w}$$

Hence

$$\frac{R}{w} = \frac{\sigma}{3(\theta + \alpha)}\left(\frac{1}{t'^2} - 1\right) \tag{19}$$

Again using figure 4

$$A = (R - D - \frac{w}{2})\cos\alpha = R\cos\theta$$

or

$$R - D - \frac{w}{2} = \frac{R\cos\theta}{\cos\alpha}$$

solving for $\frac{D}{w}$

$$\frac{D}{w} = \frac{R}{w}\left(1 - \frac{\cos\theta}{\cos\alpha}\right) - \frac{1}{2} \tag{20}$$

15

Now substituting (19) into (20)

$$\frac{D}{w} = \frac{\sigma}{3(\theta + \alpha)} \left(\frac{1}{t'^2} - 1\right)\left(1 - \frac{\cos\theta}{\cos\alpha}\right) - \frac{1}{2} \qquad (21)$$

This is the first of the required parametric equation. it reduces to the form found by Borque and Newman as shown below.

At $\alpha = 0$, (21) becomes

$$\frac{D}{w} = \frac{\sigma}{3\theta}\left(\frac{1}{t'^2} - 1\right)(1 - \cos\theta) - \frac{1}{2}$$

which is Borque's equation (15); and at $\alpha = \theta$, it red . to $-\frac{1}{2}$. (The negative sign arises from the convention that po ive D is directed away from the centerline of the jet while po ive R is directed away from the common vertex of α and θ.)

Referring to figure 1,

$$x_1 = (R - D - \frac{w}{2})\sin\alpha$$

$$x_2 = R\sin\theta$$

$$x_3 = y'/\sin\theta$$

and $\quad x = x_1 + x_2 - x_3$

Combining these yields

$$\frac{x}{w} = \frac{(R - D - \frac{w}{2})\sin\alpha}{w} + \frac{R\sin\theta}{w} - \frac{y'}{w\sin\theta} \qquad (22)$$

Substituting (17) and (19) into (22)

$$\frac{x}{w} = \frac{\sigma}{3(\theta+\alpha)}\left(\frac{1}{t'^2} - 1\right)(\sin\alpha + \sin\theta) - \frac{\tanh^{-1}}{3t'^2\sin} \quad - \left(\frac{D}{4} + \frac{1}{2}\right)\sin\alpha \qquad (23)$$

which is the second of the required parametric equations. If the value $\alpha = 0$ is used (23) reduces to

$$\frac{x}{w} = \frac{\sigma}{3\theta}\left(\frac{1}{t'^2} - 1\right)\sin\theta - \frac{\tanh^{-1}t'}{3t'^2\sin\theta}$$

which is Borque's equation (17) for the case, $\alpha = 0$.

16

Taking $\alpha = \theta$ and $\frac{D}{w} = -\frac{1}{2}$

$$\frac{x}{w} = \frac{\sigma}{3\alpha}\left(\frac{1}{t'^3} - 1\right)\sin\alpha - \frac{\tanh^{-1} t'}{3t'^3 \sin\alpha}$$

which is Borque's equation (23) for the 0 offset case assuming $\alpha = \theta$. Since $\frac{D}{w}$ is measured from the centerline, $-\frac{1}{2}$ corresponds to 0 offset.

This more general theory is expected to give more accurate results for small angles when an offset $\frac{D}{w} \geq 1$ is used, since the separation bubble will be larger and the assumption that $\alpha = \theta$ is not necessary.

2.3.4 Entrainment

The parameter σ is a floating constant that accounts for the geometrical spread of the jet due to entrainment. Previous experimental work by Reichardt (ref 4) estimated the value of σ as 7.67 for a straight jet; however, due to the curvature in this case, the entrainment, hence the value of σ, would be expected to be different. To obtain an expression for the entrained volume flow in terms of s and σ, (3) is required.

$$\left[\frac{3}{4}\frac{J(s+s_o)}{\rho\sigma}\right]^{1/2}\tanh\frac{\sigma y}{s+s_o} = \frac{Q}{2}$$

If y is taken from 0 to ∞, then $\frac{Q_T}{2}$ is equal to the total volume flow on one side of the jet centerline, including the entrained flow. Thus

$$\left[\frac{3}{4}\frac{J(s+s_o)}{\rho\sigma}\right]^{1/2}\tanh(\infty) = \frac{Q_T}{2} \tag{24}$$

or

$$\left[\frac{3}{4}\frac{J(s+s_o)}{\rho\sigma}\right]^{1/2} = \frac{Q_T}{2}$$

and since

$$J = \rho\, u_e^2\, w$$

(24) becomes

$$\frac{u_e^2}{2}\left[3\left(\frac{s+s_o}{w\sigma}\right)\right]^{1/2} = \frac{Q_T}{2} \tag{25}$$

17

Since
$$\frac{Q_e}{2} = \frac{u_e w}{2} \quad \text{from (2)}$$

and defining
$$q' = \frac{Q_T}{u_e w} = \frac{Q_T}{Q_e}$$

and substituting into (25)
$$q' = \left[3 \frac{(s + s_o)}{w\sigma}\right]^{1/2} \tag{26}$$

The entrained flow, i.e., the excess over the flow at the nozzle exit is $Q_T - Q_e$ and is normalized as

$$\frac{Q_T - Q_e}{Q_e} = q' - 1$$

At the origin $Q_e \cong Q_T$ so that the entrained flow is zero. Hence rewriting (26) as

$$q' - 1 = \left[\frac{3(s + s_o)}{w\sigma}\right]^{1/2} - 1 \tag{27}$$

yields an expression for the normalized entrained volume flow in terms of s and σ. The value of q' varies directly as s, the distance the stream travels, and inversely as σ, the spread parameter and w, the nozzle width. It also must be true that the entrained flow varies directly as the separation bubble size, since the bubble size also varies with s and σ. The separation bubble size, hence the entrainment, is determined by D/w and α. If the entrained flow is determined by s/σ, then D/w and α must affect the distance s and the spread parameter σ.

2.4 Computation

It was not possible to obtain an explicit expression for x/w as a function of α and D/w in a form that could be used for computation. Instead, parametric equations were derived and the attachment distance was computed indirectly.

First (12) and (16) give two different expressions for cos θ in terms of the parameter t' and will be referred to as the point and the volume equations, respectively. Second, (21) allows the computation of D/w, the offset distance, in terms of t', α, and σ. Finally (23) permits the computation of x/w in terms of the same quantities. For each selected value of σ and α, a range of values for t' were selected, so that θ was less than 90 deg. This required preliminary computations to

determine the range for t', since the range differed for ... point and
volume equations and for each value of σ and α used. Whe... t' ranges
were determined, the values of θ, R/w, y/w, D/w, x/w were ... d at
small intervals on each of the selected σ values and for ... ,...,
55 deg. An example of such a page of computations, which ... done on
an IBM 7090 computer, is included as table I. For each σ ... condition,
the x/w that corresponded to D/w = 0, 2, 4, 10 was found by interpolation.
The results are shown in Table II. This operation was re... d the
resulting points plotted and connected for each of the D/ ... for
α = 0 to 55 deg. Each page corresponds to a value of σ ... s, in
addition to the family of four theoretical curves, the e... l data
points. Figures 11 through 17 present the families of cu ... σ in
the range 1 to 15 for the control-volume model; and figur ... ugh
21 present the families for values of σ = 15, 20, 25, 30 ... tach-
ment-point model.

Table I. Sample Computer Print-out Sheet, σ = 2,

T'	COSΘ	SINΘ	Θ	R/w	y/w		x/w
1.4000000E-01	6.0431399E-01	7.9674625E-01	5.2820707E 01	3.6172296E 01	4.7933862E 00	1.191?	...19E 01
1.4900000E-01	6.1092300E-01	7.9169002E-01	5.2343926E 01	3.2139847E 01	4.5078318E 00	1.23?	...0E 01
1.5800000E-01	6.1751391E-01	7.8655996E-01	5.1865383E 01	2.8764836E 01	4.2550555E 00	1.052?	155676 01
1.6700000E-01	6.2408563E-01	7.8135595E-01	5.1385088E 01	2.5910683E 01	4.0297607E 00	9.240?	...72E 01
1.7600000E-01	6.3063704E-01	7.7607790E-01	5.0903054E 01	2.3476611E 01	3.8272331E 00	8.170?	...576E 01
1.8500000E-01	6.3716708E-01	7.7072570E-01	5.0419292E 01	2.1378086E 01	3.6455801E 00	7.25?	...575C 01
1.9400000E-01	6.4367465E-01	7.6529925E-01	4.9933811E 01	1.9560243E 01	3.4805377E 00	6.46?	...1496E 01
2.0300000E-01	6.5015863E-01	7.5979850E-01	4.9446624E 01	1.7973319E 01	3.3303329E 00	5.75?	9217E 00
2.114905?E-01	6.5661796E-01	7.5422334E-01	4.8957738E 01	1.6579400E 01	3.1930779E 00	5.19?	9732E 00
2.2099999E-01	6.6305152E-01	7.4857376E-01	4.8467167E 01	1.5348078E 01	3.0671938E 00	4.67?	...5E 00
2.3000000E-01	6.6945824E-01	7.4284464E-01	4.7974916E 01	1.4254730E 01	2.9513481E 00	4.21?	...146 00
2.3900000E-01	6.7583701E-01	7.3705110E-01	4.7480997E 01	1.3279245E 01	2.8444094E 00	3.82?	...570E 00
2.4799999E-01	6.8218674E-01	7.3117799E-01	4.6985648E 01	1.2405065E 01	2.7454106E 00	3.44?	...5127E 00
2.5699999E-01	6.8850634E-01	7.2523031E-01	4.6468107E 01	1.1618453E 01	2.6535206E 00	3.11?	...461E 00
2.6599995E-01	6.9479471E-01	7.1920812E-01	4.5989314E 01	1.0907937E 01	2.5680204E 00	2.82?	...5478 00
2.7499999E-01	7.0105076E-01	7.1311136E-01	4.5488806E 01	1.0263875E 01	2.4882855E 00	2.56?	...70E 00
2.8399999E-01	7.0727342E-01	7.0694011E-01	4.4986668E 01	9.6781111E 00	2.4137708E 00	2.33?	...7L 00
2.9299999E-01	7.1346155E-01	7.0069638E-01	4.4482911E 01	9.1437125E 00	2.3439982E 00	2...	...6E 00
3.0199999E-01	7.1961408E-01	6.9437423E-01	4.3977341E 01	8.6547523E 00	2.2785668E 00	1...	...7E 00
3.1099999E-01	7.2572994E-01	6.8797970E-01	4.3470564E 01	8.2061402E 00	2.2170443E 00	1.75	...6C 00
3.1999999E-01	7.3180798E-01	6.8151087E-01	4.2961987E 01	7.7936831E 00	2.1591609E 00	1.5?	...7E 00
3.2899999E-01	7.3784717E-01	6.7496783E-01	4.2451816E 01	7.4129745E 00	2.1046028E 00	1.46?	...75 00
3.3799999E-01	7.4384636E-01	6.6835064E-01	4.1940056E 01	7.0613016E 00	2.0531076E 00	1.3?	...6E 00
3.4699999E-01	7.4980450E-01	6.6165944E-01	4.1426714E 01	6.7355708E 00	2.0044405E 00	1.2?	...9E 00
3.5599999E-01	7.5572048E-01	6.5489431E-01	4.0911794E 01	6.4332451E 00	1.9583905E 00	1.2?	...5E 00
3.6499999E-01	7.6159339E-01	6.4805540E-01	4.0395303E 01	6.1520923E 00	1.9147675E 00	9.59?	1E 00
3.7399999E-01	7.6742158E-01	6.4114212E-01	3.9877244E 01	5.8901624E 00	1.8734001E 00	8.5?	7E-01
3.8299999E-01	7.7320651E-01	6.3415675E-01	3.9357622E 01	5.6456509E 00	1.8341329E 00	7.5?	7E-01
3.9199999E-01	7.7894091E-01	6.2709733E-01	3.8836442E 01	5.4170685E 00	1.7968251E 00	6.5?	1E-01
4.0099999E-01	7.8462969E-01	6.1996472E-01	3.8313706E 01	5.2030156E 00	1.7613489E 00	6.27?	57E-01
4.0999998E-01	7.9026973E-01	6.1275913E-01	3.7789420E 01	5.0022999E 00	1.7275877E 00	5.5?	1E-01
4.1899999E-01	7.9585997E-01	6.0548072E-01	3.7263347E 01	4.8136986E 00	1.6954353E 00	4.??	5E-01
4.2799999E-01	8.0139930E-01	5.9812972E-01	3.6736207E 01	4.6363619E 00	1.6647945E 00	4.2?	E-02
4.3699998E-01	8.0688663E-01	5.9070634E-01	3.6207287E 01	4.4692987E 00	1.6355765E 00	3.?	E-01
4.4599999E-01	8.1232085E-01	5.8321010E-01	3.5676828E 01	4.3117659E 00	1.6076999E 00	3.?	E-01
4.5499999E-01	8.1770090E-01	5.7564334E-01	3.5144832E 01	4.1630181E 00	1.5810898E 00	2.?	E-01
4.6399998E-01	8.2303564E-01	5.6800422E-01	3.4611303E 01	4.0223979E 00	1.5556776E 00	2.?	E-01
4.7299998E-01	8.2824403E-01	5.6029367E-01	3.4076239E 01	3.8893092E 00	1.5314001E 00	1.?	E-01
4.8199998E-01	8.3350494E-01	5.5251201E-01	3.3539645E 01	3.7632103E 00	1.5061942E 00	1.2	E-01
4.9099998E-01	8.3849730E-01	5.4465948E-01	3.3001522E 01	3.6436072E 00	1.4840211E 00	8.?	E-01
4.9999998E-01	8.4374999E-01	5.3673640E-01	3.2461869E 01	3.5300497E 00	1.4648164E 00	5.?	E-01
5.0849998E-01	8.4878192E-01	5.2874304E-01	3.1920690E 01	3.4221259E 00	1.4445397E 00	1.?	E-01
5.1799998E-01	8.5375203E-01	5.2067931E-01	3.1377982E 01	3.3194595E 00	1.4231488E 00	-1.?	E 00
5.2699997E-01	8.5865918E-01	5.1254946E-01	3.0833748E 01	3.2217047E 00	1.4046049E 00	-4.?	E 00
5.3599997E-01	8.6350231E-01	5.0434687E-01	3.0287987E 01	3.1285443E 00	1.3888723E 00	-7.?	E 00
5.4499996E-01	8.6828032E-01	4.9607389E-01	2.9740700E 01	3.0396866E 00	1.3719174E 00	-9.?	E 00

The numbers on this page are to be interpreted as whole ...
plied by a power of ten; thus 4.0999998E-01 is read .4...

Table II. Interpolated values of $\frac{x}{w}$ and θ for sel___ed $\frac{D}{r}$

D/w	x/w	
0.	-9.6919863E-01	3.1628 ⎽E 01
1.0000000E 00	1.0929889E 00	4.0564 ⎽E 01
2.0000000E 00	2.8548701E 00	4.4175 ⎽⎽ 1
4.0000000E 00	6.2584630E 00	4.7725 ⎽E 01
6.0000000E 00	9.6303045E 00	4.9605 ⎽E 01
8.0000000E 00	1.2998519E 01	5.0818 ⎽E 01
1.0000000E 01	1.6368838E 01	5.1684 ⎽E ⎽1

3. EXPERIMENTAL PROGRAM

Experiments were conducted with both air and wate_   determine
the attachment distance as a function of offset distanc_   ll angle
The test models were designed to obtain essentially twc   n   onal in-
compressible turbulent flow.

The test with a Mach 0.5 air jet was conducted wi_   distances
of 0, 2, 4, and 10 nozzle widths; the wall angle was 1_   5-deg in-
crements from 0 to 55 deg for each offset. Tests with _ r jet (simu-
lated Mach 0.5) were conducted with offset distances o_   ,_ 1c 4 nozzle
widths; and the wall angle was moved in 2-deg incremen_   _ to 40 deg
or less for each offset. The attachment distances for   and for
computer solutions of the parametric equations for vario_ vu__es of the
spread parameter σ are plotted in figures 11 through 21.

3.1 Air-Jet Test Model

The test model used in air-jet tests is show_   5. The
nozzle aspect ratio (nozzle height to width) is 8, whi_   satis-
factory approximation of two-dimensional flow, particul_   _ the
measurements are made halfway between the constraining _

The nozzle is 1/32-in. wide; the attachment v_   _0 nozzle
widths long, and can be rotated through 60 deg and offs_   as 10
nozzle widths.

The attachment point is the location on the _   all
where the stream divides, so that all fluid on one sid_   _ the bub-
ble and all fluid on the opposite side continues along _   Along
the surface of the wall, the dynamic pressure vector is _   _irection
of the stream beyond the attachment point, but back tow_   zzle within
the inclosed bubble. Therefore, the point on the surf_   _all at
which the total dynamic pressure goes through a null sh_   good

JET FLOW

LOW PRESSURE
REGION

ATTACHMENT
WALL

JET BOUNDARY

PITOT PROBE

Figure 5. Sc   ic of
experimental   jet
arrangement.

OFFSET
D

NOZZLE OPENING

PITOT TUBE

ATTACHMENT WALL
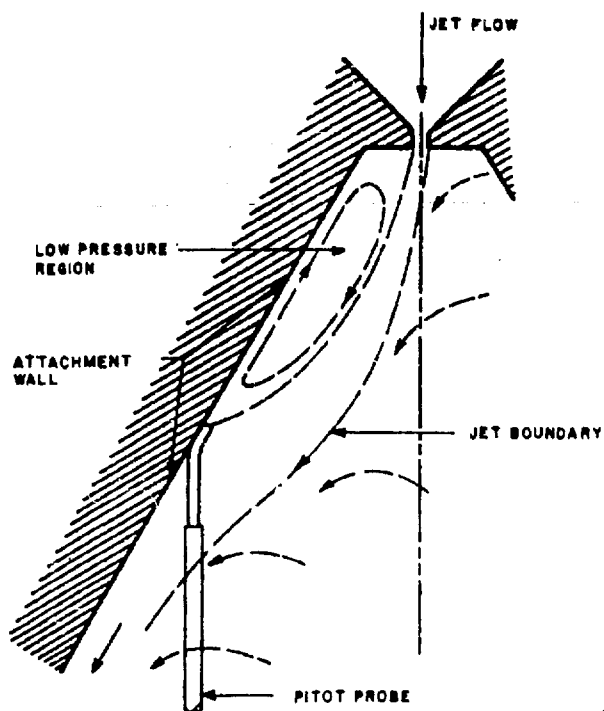
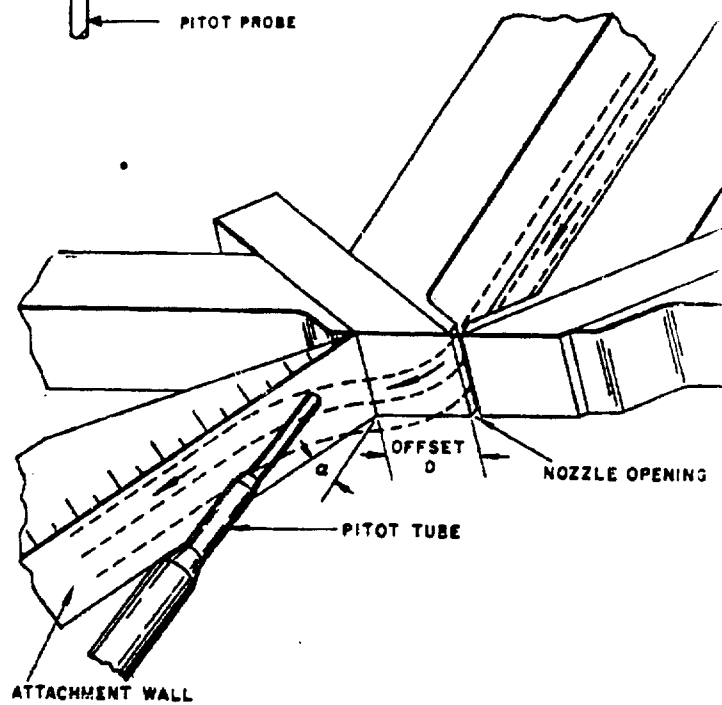Figure 6.   Isometric view of experimental air-jet   a   nt.

21

estimate of the attachment point. To determine the location of the null, a single, 0.022-in. o.d., 0.012-in. i.d. pitot tube was placed parallel to the nozzle axis and moved along the attachment wall with the pitot probe bent slightly to follow the wall. The pitot was mounted on a calibrated jeweler's three-slide rest which measured the distance along the wall, with height adjustment maintained halfway between the constraining plates as shown in figure 6. The point at which the dynamic pressure went through zero was recorded as the attachment point. The data obtained are plotted as open symbols on figures 11 and 21. This method was used in preference to static probes, which would have required moving for each test.

The output of the pitot was fed to a pressure-voltage transducer, amplified, and readout on an x-y recorder. This to be an extremely sensitive arrangement and a few thousandths of inch of pitot movement was readily detectable on the recorder. When the attachment bubble was very small, as in the case of zero offset and α, instability due to the probe size was encountered. When α was than 25 deg at zero offset, the width of the bubble was less than the probe diameter, and the attachment point could not be located.

An inherent error is associated with this method measurement, because the pitot opening is not a true point, and the a, which the attaching jet stream makes with the wall, changes.
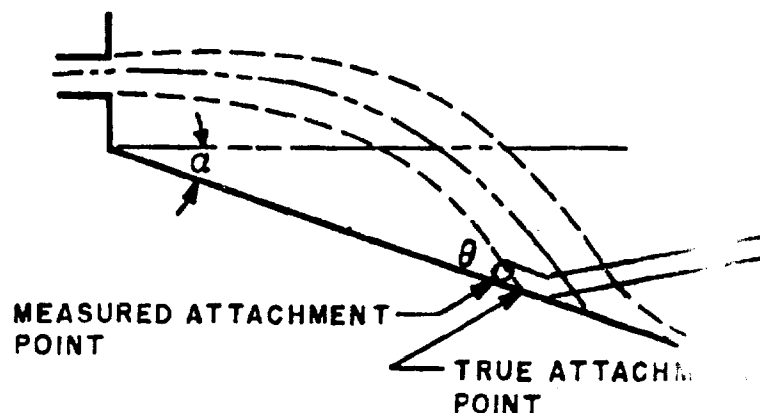

Figure 7. Errors in measuring attachment dis

The pitot tube has an opening of about 1/3 nozzle width and tends to average the high and low pressures. The smaller the angle, the greater will be the averaging, which will tend to give an apparent ater x/w than the actual value. This effect will decrease to a minimum as the attachment angle approaches 90 deg, as seen from figure 7.
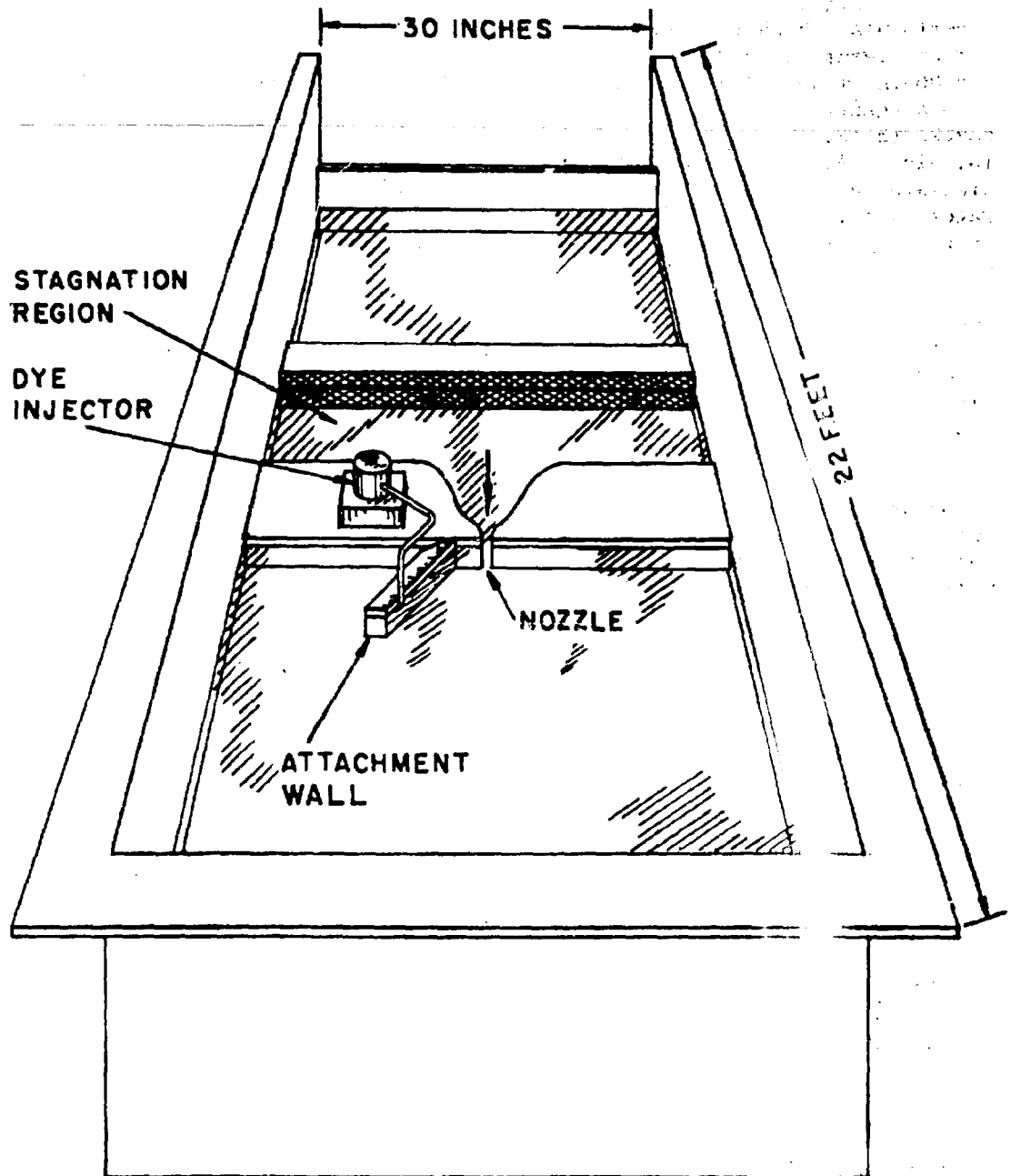
Figure 8. University of Maryland water table.

3.2 Water-Jet Test Model

Figures 8, 9, and 10 illustrate the water tab used in these experiments, which were conducted[*] at the university of ryland Wind Tunnel Operations Department (ref 5). The water table i 22 ft long and 30 in. wide. The water flow was gradually channeled from the 30-in. wide stagnation region to the nozzle throat, which was 0.5 in. wide. An estimate of the simulated Mach number on the water table, provided by the University (ref 6), is Mach number $= [2(d_0-d)/d]^{1/2}$ where d_0 = stagnation region depth, d = depth at nozzle exit. Water depth readings were recorded at the nozzle exit and stagnation region; the simulated Mach number used was 0.5

The distance along the attachment wall was measured by introducing a dye and noting the point of stagnation on the wall. The dye was introduced
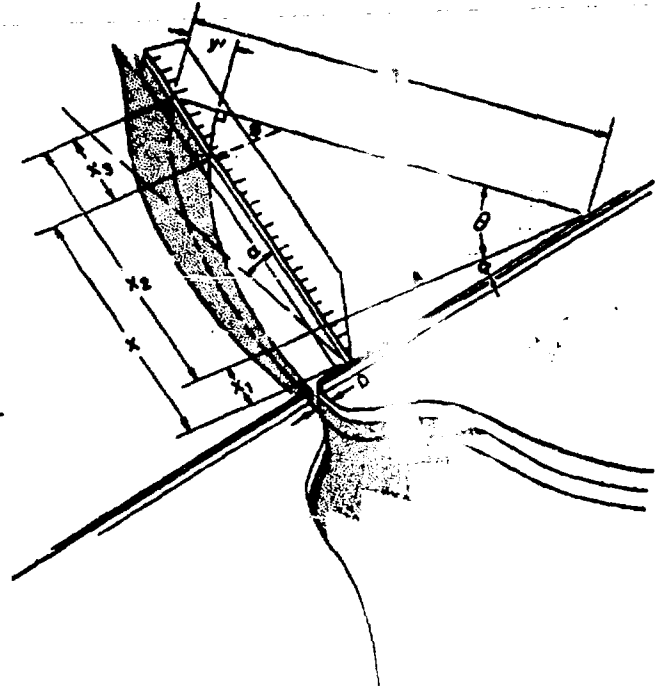

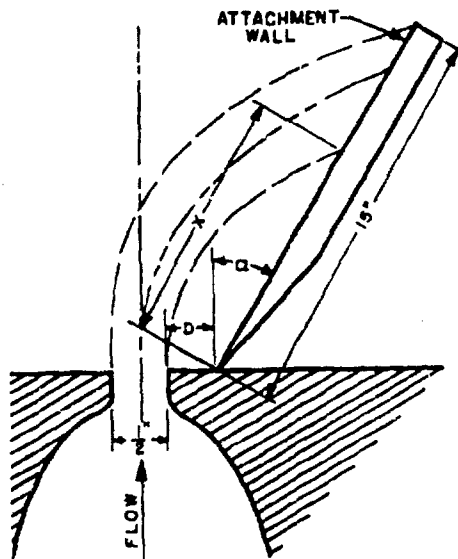Figure 9. University Maryland Water table. Mathematic model superimposed.

via a small probe placed p endicular to the water table and adjace. to the attachment wall. The water t d ta are plotted as solid symbols o l s 11 through 21. Offsets of 0, J i nozzle widths were used, and, fo fset, the attachment wall was move at 2-deg increments as far as the tabl th would permit. With the geometry en, it was impossible to increase e le α to greater than 40-deg, and e wall was only 25 nozzle widths ucing it further to obtain great was not considered.

Figure 10. Schematic of experimental water table.

24

3.3 Comparison of Results

The attachment-point equations give satisfactory agreement with the experimental results for offset distances of 0, 2, and 4 nozzle widths at values of α less than 40 deg using $\sigma = 15$ and $\sigma = 20$ (fig. 18, 19). Agreement is poor for other values of α and for an offset distance of 10 nozzle widths and does not appear to improve for other values of σ.

The control-volume computations agree with the experimental results, but a single value of σ does not fit for all conditions. If it is assumed that the value of σ for which the data and theory agree is the effective σ for the particular D/w and α, then the following observations can be made by examining figures 11 through 17: as α increases, the value of σ decreases, and as D/w increases, the value of σ decreases. The relations can be very crudely estimated as shown in the chart below.

Approximate values of σ for combinations of α and D/w

D/w \ α	0	10	20	30	40
0	-	12	10	8	6
2	12	10	8	6	4
4	10	8	6	4	2
10	2.5	1	1	1	1

These results are consistent with the development given in sec. 2.3.4; i.e., σ is a function of D/w and α hence of bubble size.

The width of the water table severely limits the wall length and the angle α through which it may turn. For the data available, it is noted that the theoretical control-volume computations for $\sigma = 7$ and 8 (fig. 14, 15) show excellent agreement with the data for D/w = 0, 2, and 4 nozzle widths over the range of possible values of α. The computations of $\sigma = 6$ agree better with the D/w = 4. The theoretical attachment-point computations agree closely with the data for D/w = 0 using a $\sigma = 15$ and for D/w = 2 and 4 using a $\sigma = 20$.

The water and air jet results show excellent agreement over the entire range. Since two different fluids, two different devices, and two different methods of measuring the attachment were used by two independent sets of experimenters, the excellent agreement is remarkable.

4. SUMMARY

Equations were developed that predict the attachment distance x/w in terms of offset D and wall angle α for a two-dimensional incompressible
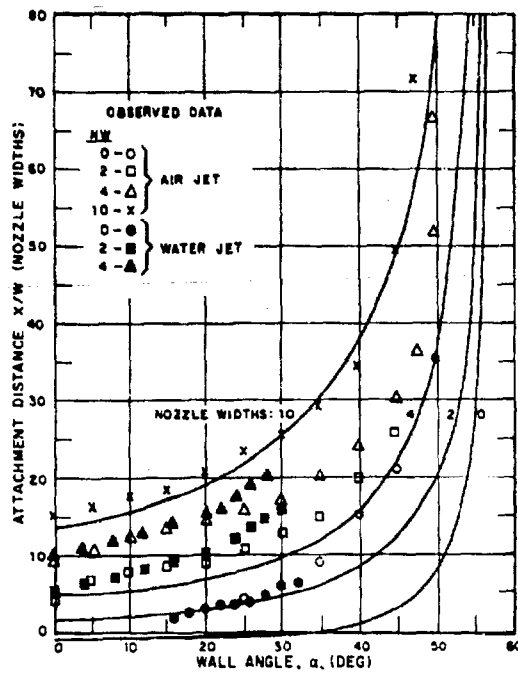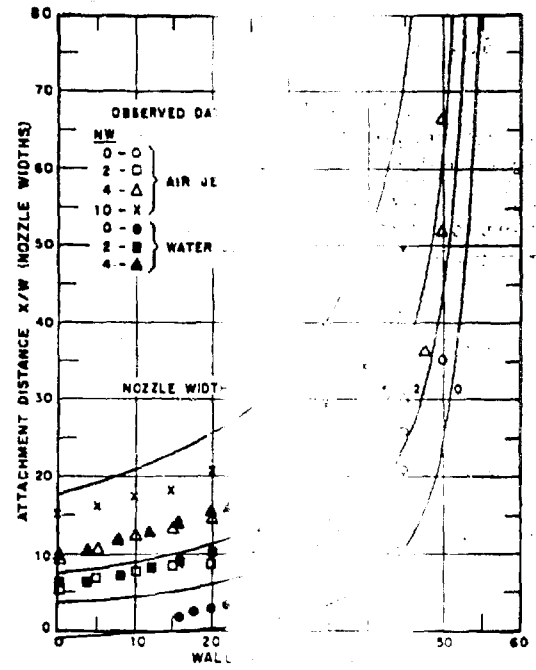
Figure 11. $\sigma = 1$

Figure 1.. ..J
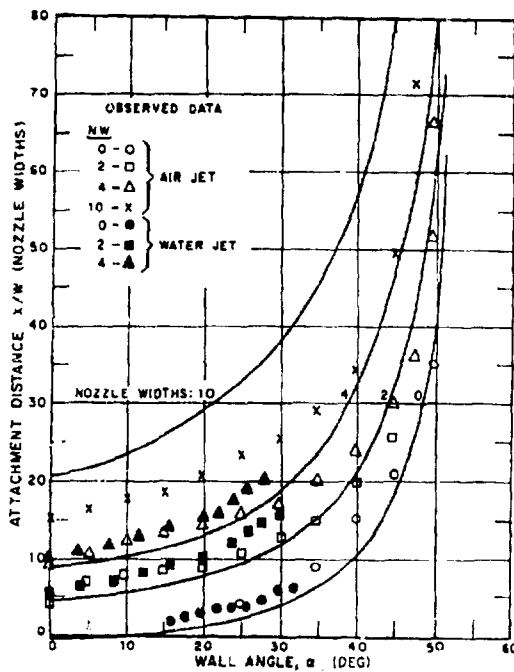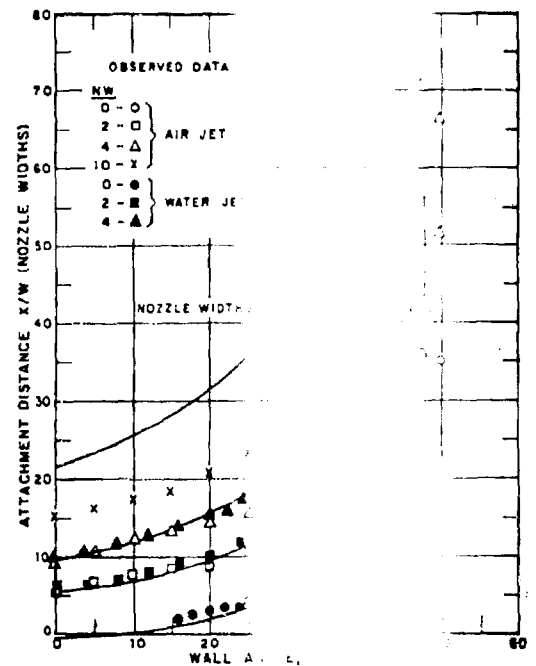

Figure 13. $\sigma = 5$

Figure 14

Figures 11 through 14. Comparison of observed att   .ces
with theoretical computations based on control

26
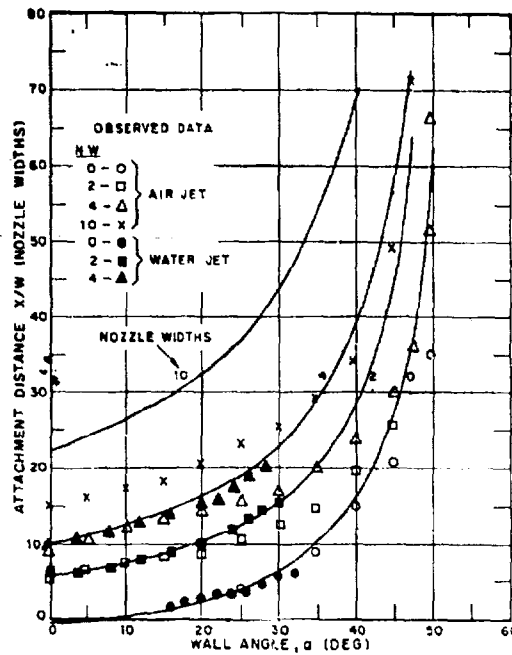
Figure 15. σ = 8
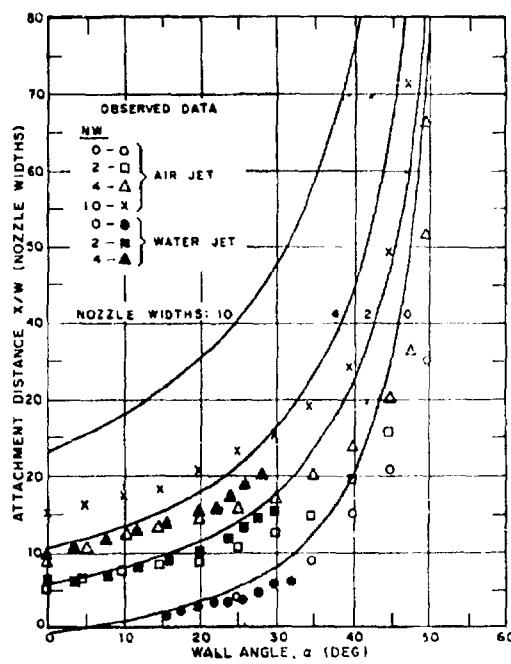

Figure 16. σ = 10
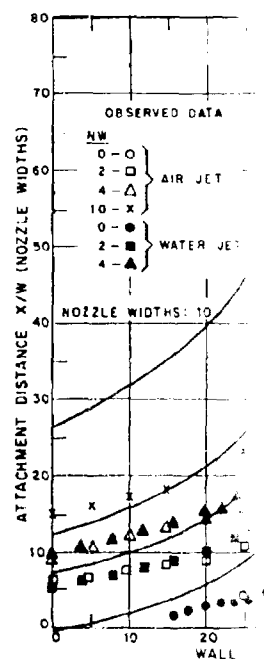

Figure 17.

Figures 15 through 17. Comparison of observed at~ ~ances
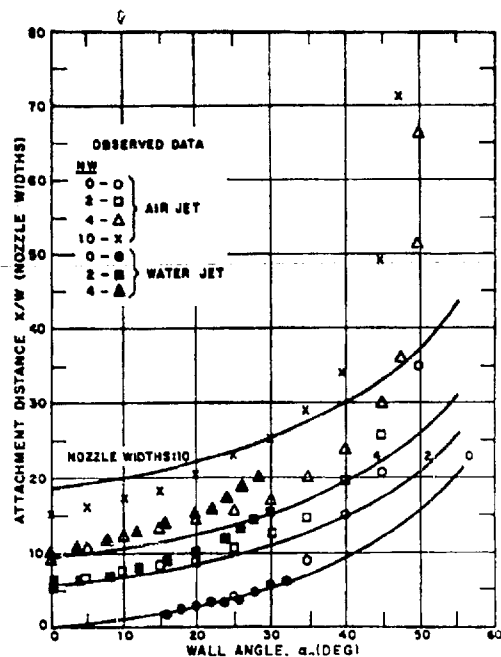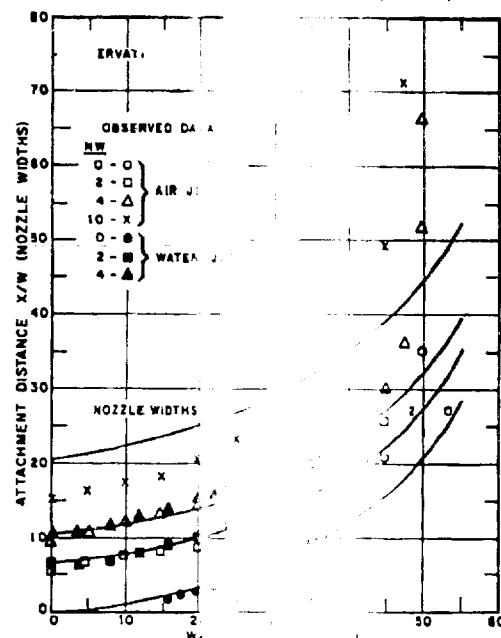with theoretical computations based on control ᵥ

27

Figure 18. σ = 15

Figure 19.
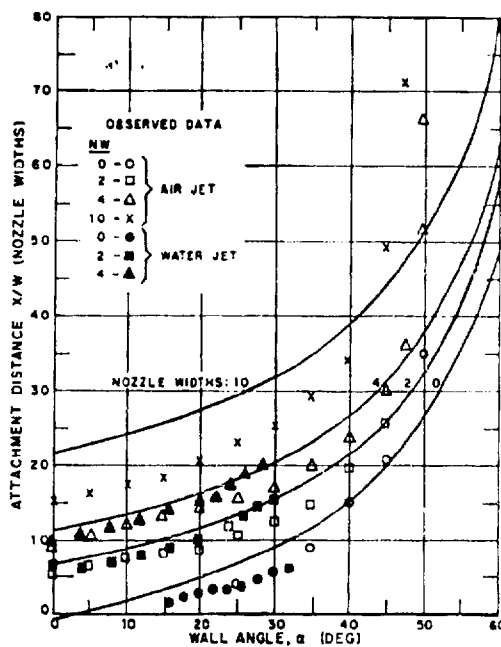

Figure 20. σ = 25
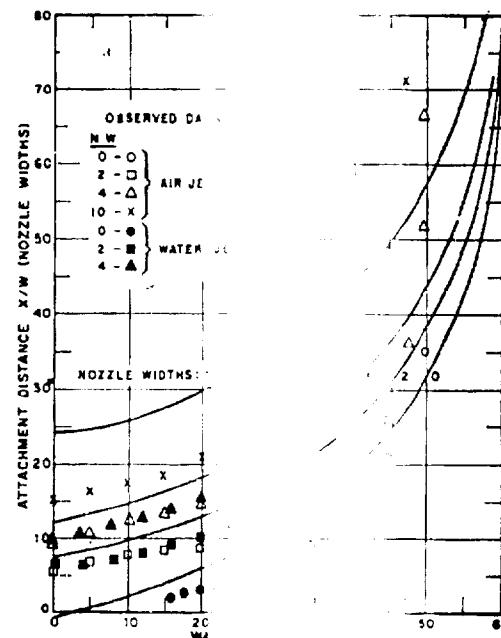

Figure 21.

Figures 18 through 21. Comparison of observed atta nces
with theoretical computations based on attachmen 1.

28

turbulent jet. The expressions are obtained in terms   r t
which is defined as

$$t = \tanh\left[\sigma y/(s+s_o)\right]$$

where y is the distance from the centerline, s is the   jet
has traveled, and σ is a spread parameter. Using two   ex-
pressions for the attachment angle θ were derived.

attachment-point model $\cos\theta = \dfrac{3}{2} - \dfrac{t'^3}{2}$

control-volume model $\cos\theta = \dfrac{1}{2} + \dfrac{3t'}{4} - \dfrac{t^\circ}{4}$

Introducing the geometry, the parametric expressions f
developed are

$$\frac{D}{w} = \frac{\sigma}{3(\theta+\alpha)}\left(\frac{1}{t'^2} - 1\right)\left(1 - \frac{\cos\theta}{\cos\alpha}\right) - \frac{1}{2}$$

and

$$\frac{x}{w} = \frac{\sigma}{3(\theta+\alpha)}\left(\frac{1}{t'^2} - 1\right)(\sin\alpha + \sin\theta)\frac{\tanh^{-1}t'}{3t'^2 \sin\theta} -   \alpha$$

Computations were performed using both expressions for   r
several values of α.

Experiments were carried out on an airjet model us   tube
to determine the attachment point for values of D/w = (nd
α = 0, 5,..., 55 deg. Similar experiments on the water   one
for D/w = 0, 2, 4, and α = 0, 2, 4, ..., 40 deg. In b
curves of x/w versus α formed distinct families that lo   e
hyperbolas with the D/w determining the location of the   nd
the α designating the position on the horizontal axis.   ntal
water jet results show excellent agreement with the con   model
computations for σ = 8 for D/w = 0, 2, and 4 over the c   re
of wall angles. The computed value of x/w for airjets
control-volume model agree with the experimentally dete
is allowed to change inversely as D/w and α. This is r   e
entrainment varies inversely as σ (27), hence entrainme   ctly
as D/w and α. Computations based on the attachment-poi   ing
values of σ = 15, and σ = 20 and for 0, 2, and 4 nozzle   n α
range of 0 to 35 deg agree with test data.

5. CONCLUSIONS

The equations developed in this report show good a   he
data obtained from water and airjet experimental data i

parameter is allowed to vary. The computations base   ntrol-
volume model showed the effective σ was inversely pr   to both
D/w and α. The variation in σ is consistent with th   at en-
trained mass flow is inversely related to σ. Using t   ont-
point model, the effective σ appears to be directly   ec   D/w and
to α. This model neglects the effect of bubble press   h   the
control volume model is the preferred analytical rep   t   . The
theoretical development requires a number of assumpti   tler's
jet profile equation is used, which assumes that the   is
that of a free jet and is constant. In this report t σ
the spread parameter is treated as a floating consta   eval-
uated by comparison with the experimental data. Furt   ht
lead to the development of equations in which σ is a   D/w
and α or of other parameters of known value.

6. REFERENCES

(1) C. Borque and B. G. Newman, "Reattachment c   nsional,
Incompressible Jet to an Adjacent Flat Plate," The A   uarterly,
Vol XI, Aug 1960, p 201

(2) R. A. Sawyer, "The Flow Due to a Two-Dimens   ssuing
Parallel to a Flat Plate," Journal of Fluid Mechanics   art 4,
p 543.

(3) H. Goertler, "Boundary Layer Theory," ed. H   ,
McGraw Hill, New York, 1960, p 605.

(4) H. Reichardt, "Gestzmossigkeiten der Freien
V. D. I., Korschungsheft, 1942, p 414

(5) A. C. Bowers, "Diffusor Side Wall Attachment   mic
Model-Subsonic Velocity," University of Maryland Wind   randum
Report No. 14, March 1961.

(6) A. C. Bowers, "The Hydraulic Analogy and it   to
the Study of Fluid Amplification Devices," University   Wind
Tunnel Memorandum Report No. 13, March 1961.

APPENDIX A.   Derivation of $R = J/\Delta p$

This equation can be arrived at using the wel   lations

$$R \omega^2 = a_n, \quad \omega = V/R$$

Writing

$$\text{normal acceleration} = \frac{\text{pressure drop} \cdot \text{area}}{\text{density} \cdot \text{volume}}$$

as

$$a_n = \frac{(p_{oo} - p_B) \cdot A}{\rho \, A \, w} = \frac{\Delta p}{\rho w}$$

Substitute into above

$$R \frac{V^2}{R^2} = \frac{\Delta p}{\rho w}$$

Simplify

$$\frac{1}{R} = \frac{\Delta p}{\rho w \, V^2}$$

Since

$$2 \, (p_o - p_{oo}) \, w = \rho V^2 w = J$$

$$R = \frac{\rho \, w \, V^2}{\Delta p} = \frac{J}{\Delta p}$$

a_n normal acceleration (ft/sec^2)

A area at the jet centerline (ft^2)

R radius of the jet curvature (ft)

V linear velocity of the jet (ft/sec)

w jet width (ft)

ρ jet density (lbm/ft^3)

ω jet angular velocity (rad/sec)

DISTRIBUTION

Office of the Director of Defense Research & Engineering
AMC Detachment No. 1, Temporary Bldg I
    Attn: Technical Library (2 copies)

Commandant
U.S. Army Artillery & Guided Missile School
Fort Sill, Okla
    Attn: Combat Development Department

Commander
U.S. Naval Ordnance Laboratory
White Oak, Silver Spring 19, Md.
    Attn: Technical Library (2 copies)

Commanding General
White Sands Missile Range
White Sands, New Mexico
    Attn: ORDES-OM, Tech Library

Commanding Officer
Watervliet Arsenal
Watervliet, New York
    Attn: Technical Library

Transportation Research Command
Ordnance Liaison Officer
Fort Eustis, Va.

Commanding Officer
Picatinny Arsenal
Dover, New Jersey
    Attn: Technical Library (3 copies)

Commanding General
Ordnance Weapons Command
Rock Island, Ill
    Attn: Technical Library

Ordnance Technical Intelligence Agency
Arlington Hall Station
Arlington 12, Virginia
    Attn: Technical Library

Commanding Officer
Ordnance Special Weapons
Ammunition Command
Dover, New Jersey
    Attn: Technical Library

33

This document contains
blank pages that were
not filmed

Commanding Officer
Ordnance Materials Research Office
Watertown Arsenal
Watertown 72, Mass.
   Attn: Director's Office

Director, Special Weapons
Office of the Chief of Research & Development
Department of the Army
Washington 25, D. C.

Commanding General
U.S. Army Electronics Proving Ground
Fort Huachuca, Arizona
   Attn: Technical Library

Director, Army Research Office
Office of the Chief of Research & Development
Department of the Army
Washington 25, D. C.
   Attn: Technical Library

Commanding Officer
Department of the Army
Springfield Armory
Springfield 1, Mass.
   Attn: TIU

Commanding Officer
AMC Detachment No. 1 Temporary Bldg 1
Washington 25, D. C.
   Attn: ORDTU
   Attn: ORDTS
   Attn: ORDTN
   Attn: ORDTB
   Attn: ORDTX
   Attn: ORDTW

Commanding General
Headquarters, U.S. CONARC
Materials Developments Section
Fort Monroe, Virginia
   Attn: MD-1

Commanding Officer
New York Ordnance District
770 Broadway
New York 3, N. Y.
   Attn: William P. Blake

Commanding Officer
Army Research Office (DURHAM)
Box CM, Duke Station
Durham, N. C.

Commanding General
U.S. Army Ordnance Missile Command
Redstone Arsenal, Alabama
     Attn: Technical Library (3 copies)
     Attn: ORDXM-REE, Bldg 7446, Charles Schriener
Commanding General
Aberdeen Proving Ground
Branch 3, Bldg 400
Aberdeen, Maryland
     Attn: Tech Library (4 copies)

U.S. Army Artillery Board
Missile Division
Fort Bliss, Texas.
     Attn: Technical Library

U.S. Naval Underwater Sound Laboratory
Fort Trumbull
New London, Conn.
     Attn: Technical Library
     Attn: Research Division, Dr. R. Berman

Department of the Navy
Chief, Office of Naval Research
Washington 25, D. C.

Department of the Navy
RRRE-3L
Bureau of Naval Weapons
Washington 25, D. C.
     Attn: S. J. German

Commander
Naval Ordnance Laboratory
White Oak, Silver Spring, Maryland
     Attn: B. Gilbert

Commander
U.S. Naval Ordnance Laboratory
Corona, California
     Attn: Technical Library

Commander
U.S. Naval Ordnance Test Station
China Lake, California
     Attn: Technical Library

Commanding Officer
U.S. Army Limited War Laboratory
Aberdeen Proving Ground, Maryland
    Attn: Lt Col J. T. Brown

Mr. W. S. Hinman, Jr.
Deputy Assistant Secretary of the Army
Research & Development
Room 3E390, The Pentagon
Washington 25, D. C.

Office of the Director of Defense
Research & Engineering
Asst. Dir of Research Engineering (Defense)
The Pentagon, Washington 25, D. C.

Institute for Defense Analysis
Gordon Rausbeck
Advanced Research Projects Div
The Pentagon,
Washington 25, D. C.

Jet Propulsion Laboratory
Pasadena, California
    Attn: Library

USCONARC
Liaison Group
The Pentagon (Rm 3E366)
Washington 25, D. C.

Office of the Director of Defense Research & Engine
AMC Detachment No. 1
Temporary Bldg I
Washington 25, D. C.
    Attn: Director of Weapons Systems Evaluation (..o   (.. 2..812)

Commander
U. S. Naval Ordnance Test Station
China Lake, California
    Attn: Technical Director

Commander
Edwards Air Force Base, California
    Attn: AFTTC(FTOOT)

Commanding Officer
Los Angeles Ordnance District
55 S. Grand Avenue
Pasadena, California
    Attn: V. V. Barker

Commanding Officer
Frankford Arsenal
Philadelphia 37, Pennsylvania
    Attn: Reference Librarian (3 copies)

Commanding General
Engineering Research & Development Laboratory
Fort Belvoir, Virginia
    Attn: Technical Library

Department of the Army
Office of the Chief of Research & Development
Washington 25, D. C.
    Attn: Chief, Combat Material Div

Department of the Army
Army Research Office
The Pentagon, Washington 25, D. C.
    . Attn: Dr. R. Watson, Office, Chief of R & D

Commanding General
OTAC
Detroit Arsenal
Centerline, Mich
    Attn: Technical Library

Commandant
Command & General Staff College
Archives
Fort Leavenworth, Kansas

Commanding Officer
Chemical Warfare Laboratories
Army Chemical Center, Md.
    Attn: Technical Library

Commanding Officer
Army Biological Laboratories
Fort Detrick, Frederick, Md.
    Attn: Technical Library

Commanding Officer
U.S. Army Signal Research & Development Laboratory
Fort Monmouth, N. J.
    Attn: Technical Library
    Attn: Arthur Daniel

Commander
Naval Research Laboratory
Washington 25, D. C.
    Attn: Technical Library

Commandant
U.S. Marine Corps
Code A04F
Washington 25, D. C.

Department of the Navy
Bureau of Naval Weapons
Washington 25, D. C.
    Attn: Code CACF-3

Department of the Navy
Chief of Naval Operations
R & D Planning Group
The Pentagon, Washington 25, D. C.

Commander
Aeronautical Systems Division
Wright-Patterson Air Force Base, Ohio
    Attn: Technical Library

Department of the Air Force
Deputy Chief of Staff for Development
Director of R & D
The Pentagon, Washington 25, D. C.

Commander
Armed Services Technical Information Agency
Arlington Hall Station
Arlington 12, Virginia
    Attn: TIPDR (10 copies)

Commander
Armed Services Technical Intelligence Agency
Arlington Hall Station
Arlington 12, Virginia
    Attn: TIPDR-B

Commander
Air Research & Development Command
Andrews Air Force Base
Washington 25, D. C.
    Attn: Technical Library - B

Commander
Air Proving Ground Center
Eglin Air Force Base, Florida
    Attn: Technical Library

Commander
Air Material Command
Wright-Patterson Air Force Base, Ohio
    Attn: LMDN

Air Force Systems Command
Space Systems Division
Los Angeles 45, California
    Attn: Technical Data Center

Commander
Air Force Ballistic Missile Division
Inglewood, California
P.O. Box 262
    :Attn: WDSOT

Air Force Special Weapons Center
Kirtland Air Force Base
Albuquerque, New Mexico

Aeronautical Systems Division
Wright-Patterson Air Force Base, Ohio
    Attn: WWRMOO (M. Schorr)

Scientific and Technical Information Facility
P. O. Box 5700
Bethesda, Maryland
    Attn: NASA Representative (S-AK/DL)
National Aeronautics & Space Administration
Langley Research Center
Langley, Station, Hampton, Va.
    Attn: Technical Library

National Aeronautics & Space Agency
Lewis Research Center
2100 Brookpart Road
Cleveland 35, Ohio
    Attn: K. Hiller

Marshall Space Flight Center
Advanced Propulsion Section
Huntsville Alabama
    Attn: M-S&M-PA

Marshall Space Flight Center
Computation Division
Huntsville, Alabama
    Attn: Dr. Walter P. Krause

Chief, Defense Atomic Support Agency
Washington 25, D. C.
    Attn: DASAG/Library

U.S. Atomic Energy Commission
Washington 25, D. C.
    Attn: Technical Reports Library

U.S. Atomic Energy Commission
Division of Military Applications
Germantown, Md.

Advisory Group on Elec Ts
Mcore School Building
200 S. 33rd St.
Philadelphia 4, Pennsylvania
    Attn: Allan M. H

Director
Advanced Research Projects Agency
Washington 25, D. C.
    Chief, Technical Operations Division

Atomic Energy Commission
Space Nuclear Propulsion ffice
Washington 25, D. C.
    Attn: F. C. Schwe

University of Maryland
Director, Wind Tunn
College Park, Maryland
    Attn: Donald S.

United Aircraft Corporation
Research Division
East Hartford 8, Connecticut
    Attn: Mr. R. Ol n

Los Alamos Scientific Laboratory
Los Alamos, New Mexico
    Attn: Library

U.S. Library of Congress
Washington 25, D. C.
    Attn: Science logy Division

Army Engineer Research & Development Laboratories
Fort Belvoir, Virginia
Attn: Chief, Mechanical Dept

University of New Mexico
Albuquerque, New Mexico
Attn: Dr. Richard Moore

University of Michigan
Institute of Science & Technology
2038 E. Engr Bldg
Ann Arbor, Mich
Attn: R. R. White, Director

University of Maryland
College of Aeronautical Engineering
College Park, Maryland
Attn: W. Sherwood

University of Florida
Physics Department
Gainesville, Florida
Attn: Technical Library - Alex G. Smith
Attn: L. H. Roberts

Engineering Library
University of California
405 Hilgard Avenue
Los Angeles 24, California
Attn: Mrs. J. E. Tallman

Engineering Library
University of California
Berkeley, California
Attn: Mrs. Blanche Dalton

University of Arizona
Physics Department
Tucson, Arizona
Attn: Professor Ulrich H. Bentz

Sandia Corporation
Sandia Base
Albuquerque, New Mexico
Attn: Technical Library

Rensselaer Polytechnic Institute
Dept of Aeronautical Engineering
Troy, New York
    Attn: Mr. K. T. Yen

Patent Office
Washington 25, D. C.
    Attn: Scientific Library

Ohio State University
576 Melrose Avenue
Columbus 2, Ohio
    Attn: Technical Library

New York Naval Shipyard
Bldg 291, Code 912B
Brooklyn 1, New York
    Attn: Library

National Physical Laboratory
Teddington, Middlesex, England
    Attn: Technical Library
    Thru: AMC Detachment No. 1, Washington 25, D. C.
        Attn: CIDTN

National Bureau of Standards
Bldg 16 - Rm 310
Washington 25, D. C.
    Attn: Chief Secti   1.06

National Bureau of Standards
Boulder, Colorado
    Attn: Technical Library

National Bureau of Standards
Washington 25, D. C.
    Attn: Library

Minneapolis-Honeywell Regulator Company
2753 Fourth Avenue, C.
Minneapolis 8, Minn.
    Attn: Mr. H. Sparrow

Massachusetts Institute of Technology
Dept of Mechanical Engineering
Cambridge, Mass.
    Attn: L. Shearer

Linda Hall Library
Joseph C. Shipman
5109 Cherry Street
Kansas City 10, Miss   1

Johns Hopkins University
Applied Physics Laboratory
8621 Georgia Avenue
Silver Spring, Maryland
      Attn: Tech Library (2 copies)

Franklin Institute of the State of Pennsylvania
Philadelphia 3, Pennsylvania
      Attn: C. W. Harg s, Tech Director

Mr. Charles A. Belsterling
Franklin Institute of the State of Pennsylvania
Philadelphia 3, Pennsy ania

Engineering Societies   rary
29 W. 39th Street
New York 18, New York
      Attn: Mr. John H   ng, Order Librarian

Dayton & Montgomery Co   y Public Library
215 East Third Street
Dayton 2, Ohio
      Attn: Circulation   artment

Corning Glass Works
Corning, New York
      Attn: James K. D

Cornell University
Ithaca, New York
      Attn: Dr. Ed Res   Jr.

John Crerar Library
86 E. Randolph Street
Chicago 1, Illinois
      Attn: H. Henkle

Battelle Memorial Insti
Chief Systems Engr Div
505 King Avenue
Columbus 1, Ohio
      Attn: Chief Syste   Engr. Div.

Armour Research Foundat   of Illinois Ins. of Tech
10 W 45th Street
Chicago 16, Ill
      Attn: Mr. George   . Jacobi

Rutgers University
College of Engineering
New Brunswick, N. J.
    Attn: Technical Library

New York State University
School of Engineering
6 Chemistry Road
Buffalo 14, New York
    Attn: Technical Library

Carnegie Institute of Technology
Pittsburgh, Pa.
    Attn: Technical Library
    Attn: Dr. E. . Williams

Internal

Horton, B.M./McEvoy, R.W., Lt Col
  Apstein, M./Gerwin, H.L./Guarino, P.A./Kalmus, H. P.
  Spates, J.E./Schwenk, C.C.
Hardin, C.D., Lab 100
Sommer, H., Lab 200
Hatcher, R.D., Lab 300
Hoff, R.S., Lab 400
Nilson, K., Lab 500
Flyer, I.N., Lab 600
Campagna, J.H./Apolenis, C.., Div 700
DeMasi, R., Div 800
Landis, P.E./Lab 900
Seaton, J.W., 260
Keller, C., 300
Kirshner, J., 310   (15 copies)
Warren, R., 310
Woodward, K., 310
Barclay, R., 310
Burton, W., 310
Carter, V., 310
Campagnuzolo, C.J., 310
Cuneo, W., 310
Deadwyler, R., 310
Dockery, R., 310
Fine, J.., 310
Foxwell, J., 310
Gaylord, W., 310
Goto, J., 310
Gottron, R., 310
Holmes, A., 310
Iseman, J., 310
Joyce, J., 310
Katz, S., 310
Keto, J., 310
Marsh, D., 310
Mon, G., 310
Palmisano, R., 310
Straub, H., 310
Spyropoulos, C., 310
Raviliou s, F., 310
Roffman, G., 310
Toda, K., 310
Talkin, A., 310
Wayne, S., 310
Wright, E., 310
Rotkin, I./Godfrey, T.B./Eichberg, R.L.
Bryant, W .T./Distad, M.F./McCoskey, R.E./Moorhead, J.G.
Technical Reports Unit, 800 (5 copies)
Technical Information Office, 010 (10 copies)
HDL Library (5 copies)

Eise.   10
Garvo1   .
Scudde   )
Wagn
Harri
Levi   copies)

45

AD

Harry Diamond Laboratories, Washington 25, D. C.

1. Jets and Attachment
2. Fluid Mechanics
3. Fluid Flow
4. Subsonic Flow

FLUID AMPLIFICATION—5. JET ATTACHMENT DISTANCE AS A FUNCTION OF ADJACENT WALL OFFSET AND ANGLE—Sheldon G. Levin, Francis M. Manion

TR-1087, 31 December 1962, 24 pages text, ll illus. Department of the Army Proj 5M03-01-003, OMS Code 5010.11.71800, DOFL Proj. 31100, UNCLASSIFIED Report

Attachment of a submerged, incompressible, two-dimensional, turbulent jet to an adjacent straight wall (Coanda effect) is analyzed ... t predict the point at which ... angle and offset distance. ... veral sets of conditions.

Experiments were conducted with both air and water jets at Mach 0.5 equivalent, and results agree well with corresponding computer solutions when the jet spread parameter is also treated as a function of offset distance and wall angle. The equations provide an analytic method, independent of the particular fluid, for predicting the attachment distance, and should be helpful in designing elements based on the Coanda effect; e.g., the fluid flip-flops or bistable elements.

AD

Harry Diamond Laboratories, Washington 25, D. C.

1. Jets and Attachment
2. Fluid Mechanics
3. Fluid Flow
4. Subsonic Flow

FLUID AMPLIFICATION—5. JET ATTACHMENT DISTANCE AS A FUNCTION OF ADJACENT WALL OFFSET AND ANGLE—Sheldon G. Levin, Francis M. Manion

TR-1087, 31 December 1962, 24 pages text, ll illus. Department of the Army Proj 5M03-01-003, OMS Code 5010.11.71800, DOFL Proj. 31100, UNCLASSIFIED Report

Attachment of a submerged, incompressible, two-dimensional, turbulent jet to an adjacent straight wall (Coanda effect) is analyzed ... to predict the point at which ...

Computer solutions were obtained for several sets of conditions. Experiments were conducted with both air and water jets at Mach 0.5 equivalent, and results agree well with corresponding computer solu-

---

AD

Harry Diamond Laboratories, Washington 25, D. C.

1. Jets and Attachment
2. Fluid Mechanics
3. Fluid Flow
4. Subsonic Flow

FLUID AMPLIFICATION—5. JET ATTACHMENT DISTANCE AS A FUNCTION OF ADJACENT WALL OFFSET AND ANGLE—Sheldon G. Levin, Francis M. Manion

TR-1087, 31 December 1962, 24 pages text, ll illus. Department of the Army Proj 5M03-01-003, OMS Code 5010.11.71800, DOFL Proj. 31100, UNCLASSIFIED Report

Attachment of a submerged, incompressible, two-dimensional, turbulent jet to an adjacent straight wall (Coanda effect) is analyzed ...

AD

Harry Diamond Laboratories, Washington 25, D. C.

1. Jets and Attachment
2. Fluid Mechanics
3. Fluid Flow
4. Subsonic Flow

FLUID AMPLIFICATION—5. JET ATTACHMENT DISTANCE AS A FUNCTION OF ADJACENT WALL OFFSET AND ANGLE—Sheldon G. Levin, Francis M. Manion

TR-1087, 31 December 1962, 24 pages text, ll illus. Department of the Army Proj 5M03-01-003, OMS Code 5010.11.71800, DOFL Proj. 31100, UNCLASSIFIED Report

Attachment of a submerged, incompressible, two-dimensional, turbulent jet to an adjacent straight wall (Coanda effect) is analyzed ...

Experiments were conducted with both air and water jets at Mach 0.5 equivalent, and results agree well with corresponding computer solu-

---